Nuclear Materials and Energy 34 (2023) 101393

Contents lists available at ScienceDirect

Nuclear Materials and Energy

journal homepage: www.elsevier.com/locate/nme

Influence of fatigue precracking and specimen size on Master Curve fracture toughness measurements of EUROFER97 and F82H steels[1]

Xiang (Frank) Chen [a,*], Marta Serrano [b], Rebeca Hernández [b], Dan Lu [c], Mikhail A. Sokolov [a], Sehila M. Gonzalez De Vicente [d], Yutai Katoh [a]

[a] Materials Science and Technology Division, Oak Ridge National Laboratory, PO Box 2008, Oak Ridge, TN 37831, USA
[b] Materials for Energy Interest Division, CIEMAT, Avda. Complutense 40, 28040 Madrid, Spain
[c] Computational Sciences & Engineering Division, Oak Ridge National Laboratory, PO Box 2008, Oak Ridge, TN 37831, USA
[d] International Atomic Energy Agency, Wagramer Str. 5, 1220 Wien, Austria

ARTICLE INFO

Keywords:
Small specimen test techniques
Specimen size effects
Fracture toughness
Reduced activation ferritic-martensitic steel
Master curve
Fusion

ABSTRACT

EUROFER97 and F82H steels are two leading reduced-activation ferritic-martensitic (RAFM) steels for fusion first wall and blanket applications. Exposure to the harsh environment of fusion reactors can result in severe degradation of fracture toughness. Thus, the post-irradiation evaluation of fracture toughness is critical for understanding the material behavior. Due to the space constraints of irradiation facilities and challenges in controlling a uniform irradiation condition for large size specimens, the development of small specimen test techniques (SSTT) is indispensable to evaluate the performance of irradiated materials. In this study, we evaluated specimen size effects on the Master Curve fracture toughness of EUROFER97 and F82H steels. A wide variety of specimens, including 0.5 T compact tension (C(T)) specimens, 0.16 T mini-compact tension (miniC(T)) specimens, and 1.65 mm miniature bend bar specimens, were tested. The testing methodology was based on the Master Curve method in the ASTM E1921 standard. No specimen size effect was observed in 0.5 T C(T) and 0.16 T miniC(T) specimens on the Master Curve reference temperature T_0, while 1.65 mm miniature bend bar specimens yielded a higher T_{0Q}. A strong effect of fatigue precracking on T_0 for 0.5 T C(T) and 0.16 T miniC(T) specimens was observed, such that testing on specimens with skewed fatigue precrack fronts resulted in lower T_0 than for specimens with ASTM standard qualified straight fatigue precrack fronts. The results highlight the importance of experimental quality control in developing SSTT for Master Curve fracture toughness testing. Lastly, we also evaluated and provided recommendations on the minimum number of specimens needed for each specimen type for yielding reliable T_{0Q} values.

1. Introduction

EUROFER97 and F82H are two reference reduced-activation ferritic-martensitic (RAFM) steels from Europe and Japan, respectively. Both steels have favorable properties for fusion first wall and blanket structure applications [1–5], such as reduced activation, superior swelling resistance, good thermal conductivity, and favorable fracture toughness. However, exposing materials to the harsh environment of a fusion reactor, characterized by 14 MeV neutrons, will result in both irradiation damage and He/H transmutation in the material [6], which could result in a significant degradation of material fracture toughness properties. Therefore, the post-irradiation evaluation of RAFM steel fracture toughness is critical to understand the material degradation behavior to ensure the safe long-term operation of a fusion reactor [7]. Due to the space constraints of existing test reactors and future fusion neutron sources, as well as higher costs and challenges in controlling and maintaining a uniform irradiation condition for large size specimens, the development of small specimen test techniques (SSTT) is indispensable

[1] Notice: This manuscript has been authored by UT-Battelle, LLC, under contract DE-AC05-00OR22725 with the US Department of Energy (DOE). The US government retains and the publisher, by accepting the article for publication, acknowledges that the US government retains a nonexclusive, paid-up, irrevocable, worldwide license to publish or reproduce the published form of this manuscript, or allow others to do so, for US government purposes. DOE will provide public access to these results of federally sponsored research in accordance with the DOE Public Access Plan (https://energy.gov/downloads/doe-public-access-plan).

* Corresponding author at: P.O. Box 2008, Building 4500S MS-6136, Oak Ridge, TN 37831-6136, USA.
E-mail address: chenx2@ornl.gov (X.(F. Chen).

https://doi.org/10.1016/j.nme.2023.101393
Received 12 January 2023; Received in revised form 9 February 2023; Accepted 15 February 2023
Available online 20 February 2023

Table 1
Compositions of EUROFER97 batch-3 [9] and F82H-BA12 (wt%).

	Cr	C	Mn	V	W	Ta	Si	O	N
EUROFER97 batch-3	9.47	0.10	0.48	0.21	1.14	0.11	0.03	0.0012	0.0395
F82H-BA12	7.88	0.10	0.45	0.19	1.78	0.09	0.10	0.0012	0.0098

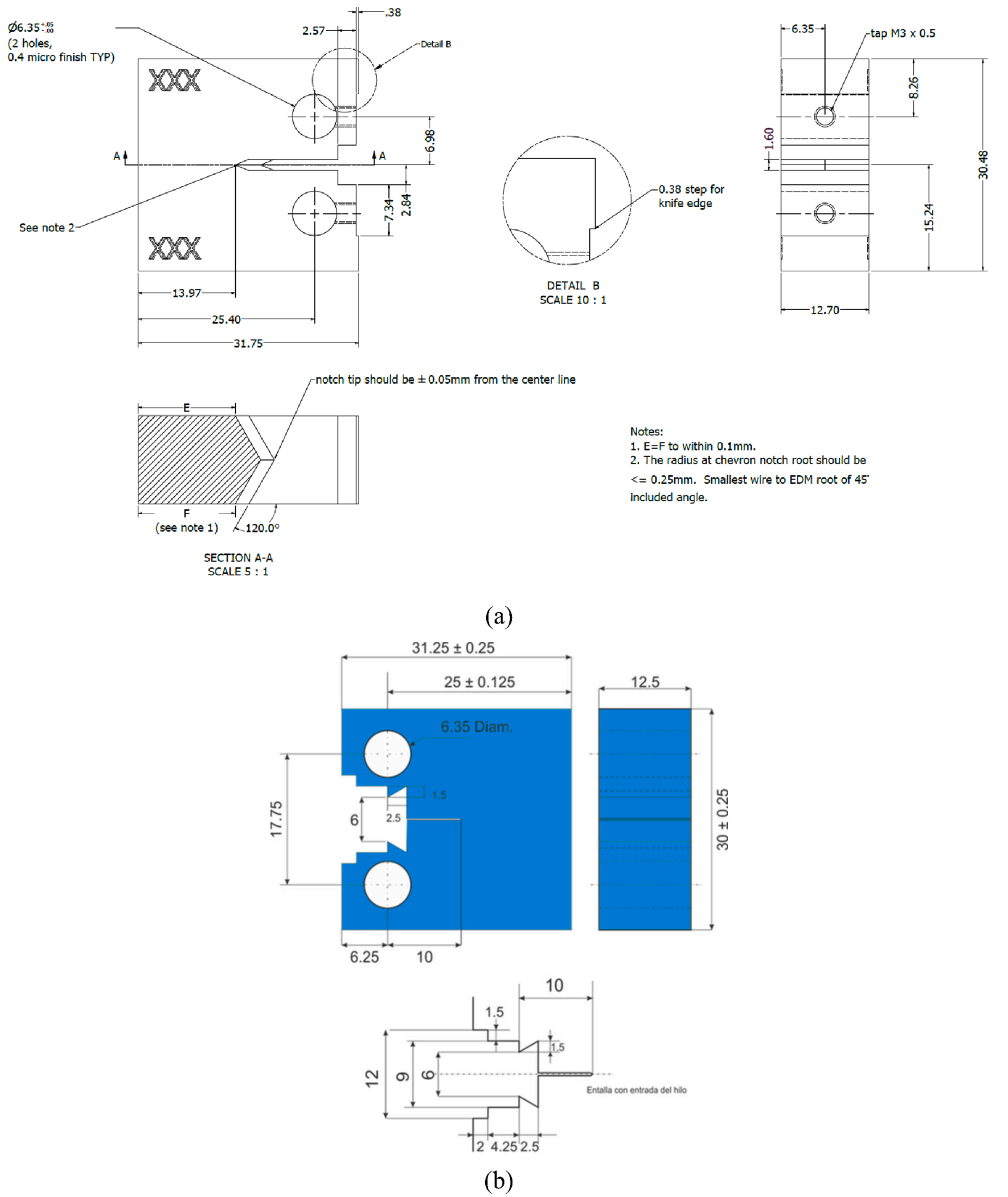

Fig. 1. Specimen drawings for ORNL 0.5 T C(T) in (a), CIEMAT 0.5 T C(T) in (b), 4 mm miniC(T) in (c), and 1.65 mm bend bar in (d). Dimensions in mm.

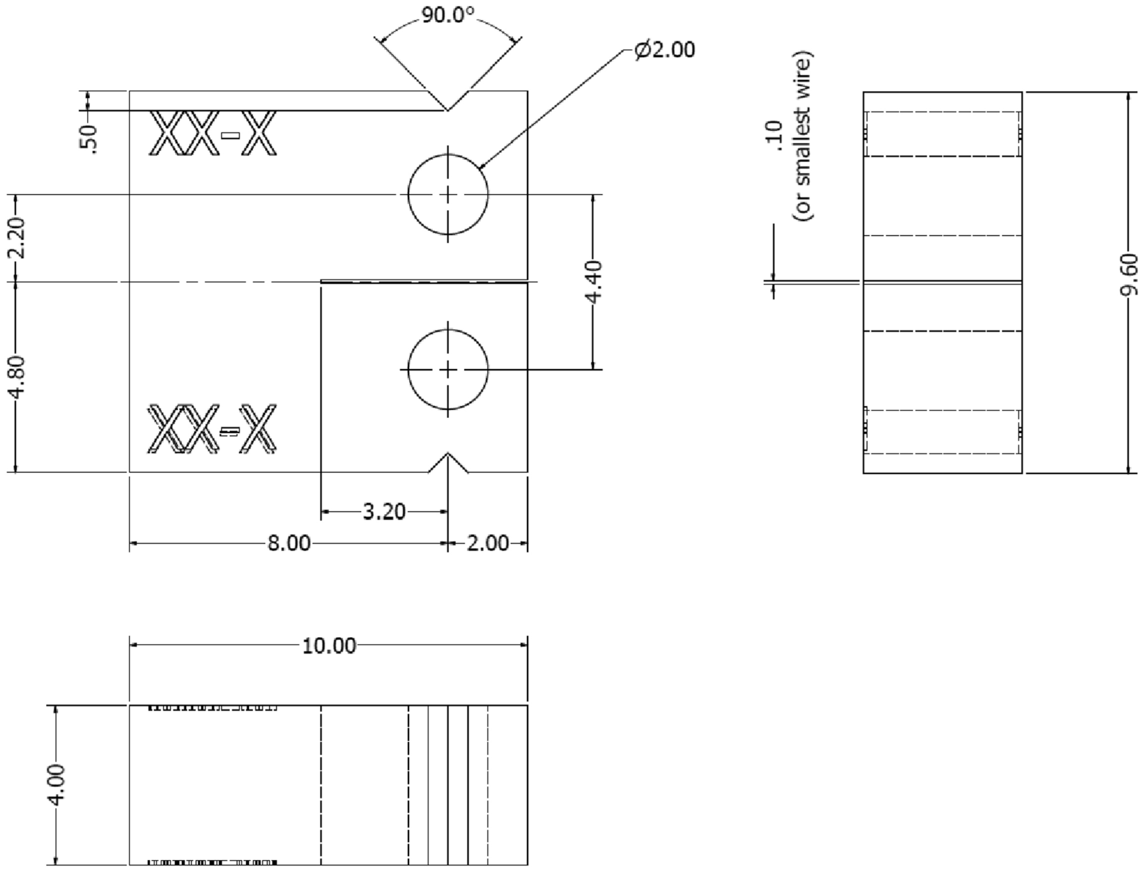

(c)

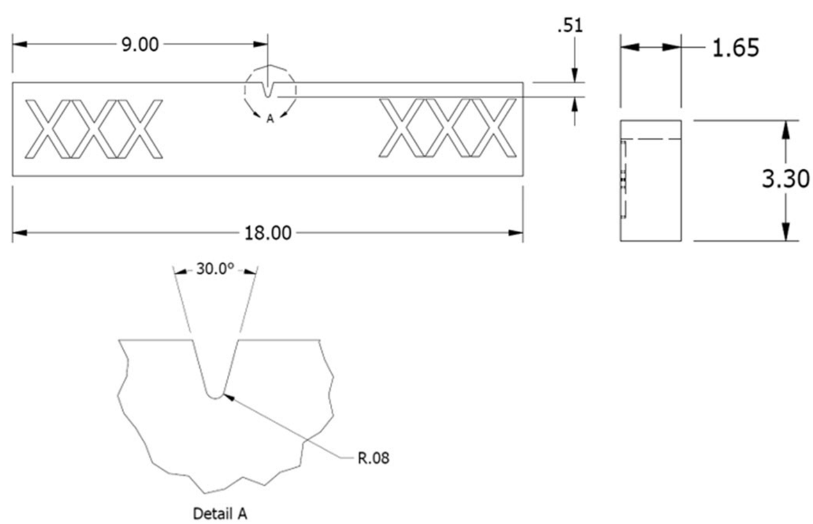

(d)

Fig. 1. (*continued*).

to evaluate the performance of irradiated materials. Under the auspices of the International Atomic Energy Agency (IAEA), a Coordinated Research Project (CRP) titled "Towards the Standardization of Small Specimen Test Techniques for Fusion Applications" has started since 2017. The overall objective of the project is to provide a set of guidelines for SSTT based on commonly agreed best practices for five mainstream test techniques: tensile, creep, low cycle fatigue, fracture toughness, and fatigue crack growth rate. The project intends to act as a first step towards a full standardization of SSTT for testing and qualifying fusion structural materials. As participants in this project, Oak Ridge National Laboratory (ORNL) and the Centre for Energy, Environmental and Technological Research (CIEMAT) performed interlaboratory fracture toughness testing based on the Master Curve method in the ASTM E1921-21 standard [8]. This paper summarizes our key findings

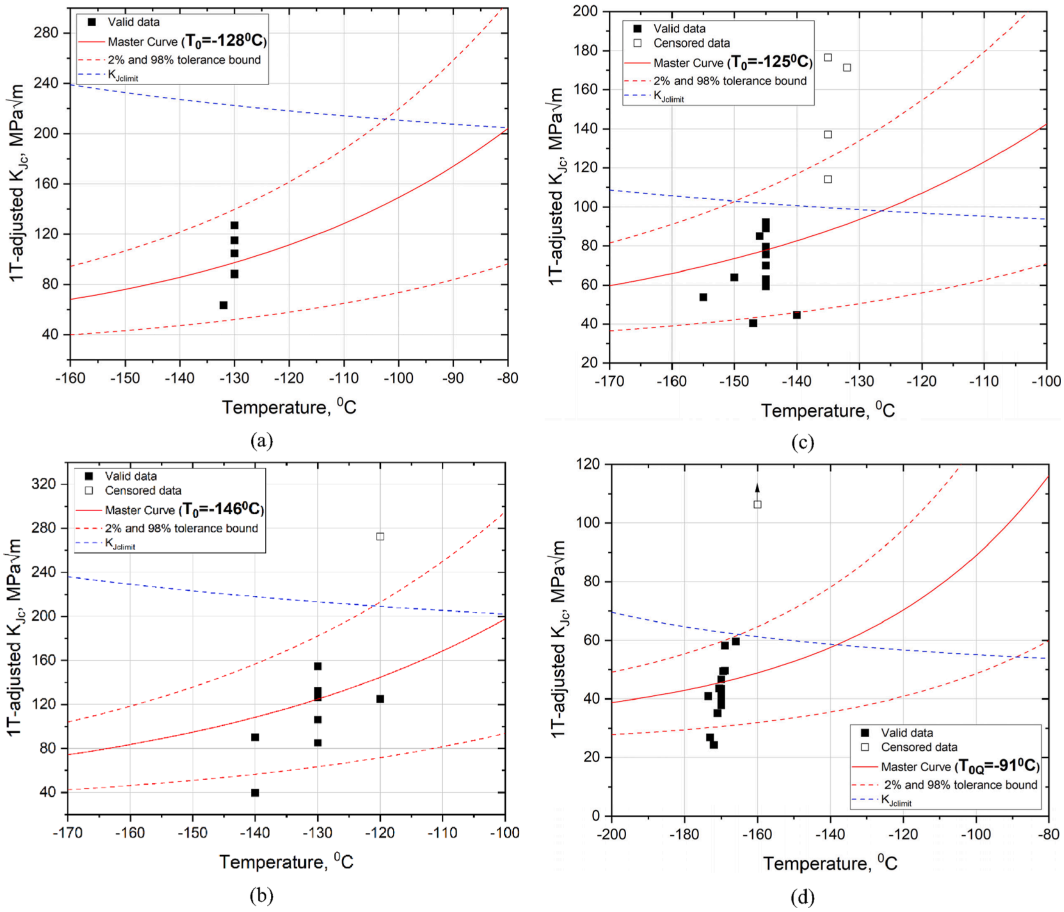

Fig. 2. Master curve fracture toughness results for EUROFER97 batch-3 (a) ORNL 0.5 T C(T), (b) CIEMAT 0.5 T C(T) (c) 4 mm miniC(T), and (d) 1.65 mm bend bar.

concerning fatigue precracking and specimen size effects on Master Curve fracture toughness characterization of EUROFER97 and F82H steels. We also evaluate and provide recommendations on the minimum number of specimens needed for each specimen type for obtaining reliable T_0 values.

2. Materials and method

2.1. Materials and specimens

Two plates of EUROFER97 batch-3 (heat 33307/07-097) and F82H-BA12 were used for fracture toughness testing. The compositions of both steels are shown in Table 1 [9,10]. The heat treatment for EUROFER97 batch-3 was austenization at 980–1040 °C for 27–30 min, followed by tempering at 750–760 °C for 90–120 min [11]. The heat treatment for F82H-BA12 was normalization at 1040 °C for 40 min followed by tempering at 750 °C for 60 min.

Three types of specimens, 0.5 T compact tension (C(T)), 4 mm mini-compact tension (miniC(T)), and 1.65 mm bend bars, were machined from the middle thickness region of supplied plates [12]. The specimen drawings are shown in Fig. 1. All specimens were machined in L-T orientation, i.e., with the crack plane normal to the rolling direction of the raw material and the crack propagation parallel to the transverse direction of the raw material.

2.2. Experimental setup

Detailed descriptions of the ORNL testing equipment can be found in Refs. [10,12–17] and are briefly summarized here. Fatigue precracking was performed on a 44.5 kN capacity servo-hydraulic frame with calibrated load cells. Depending on the specimen geometry, dedicated fixtures, grips, and deflection gauges were used for each specimen type. A commercial automated fatigue crack growth testing software was used with real-time compliance-based crack size measurement to control the fatigue precrack process. The ensuing fracture toughness testing was performed on a 97.87 kN capacity servo-hydraulic frame with calibrated load cells. Liquid nitrogen was used to control the testing temperatures, which were measured directly from a type-T thermocouple spot welded to specimens. An environmental chamber was used to enclose the specimens and the test fixture to ensure that the testing temperatures were within a ± 2.5 °C range from the target testing temperature.

CIEMAT precracking and fracture toughness tests were performed on an MTS servo-hydraulic testing machine with a load capacity of 100 kN. Fracture toughness tests were performed inside an environmental chamber and the test temperature was monitored by a type-T thermocouple attached to the specimen.

2.3. Test procedures

Specimens were fatigue precracked to the target crack size and then tested without additional side-grooving based on the Master Curve method described in the ASTM E1921-21 standard [8]. Fatigue precracking was conducted using a high frequency sinusoidal waveform under stress intensity factor K control with a fatigue stress ratio R = 0.1. For 0.5 T C(T) specimens, a decreasing K was used while for 4 mm miniC(T) specimens and 1.65 mm bend bars, a constant K was used. Per ASTM E1921, the following requirements were met during fatigue precracking:

The applied stress intensity was within the envelope of allowable maximum stress intensity factor K_{max} (See ASTM E1921-21 Fig. 6 and Table 1).

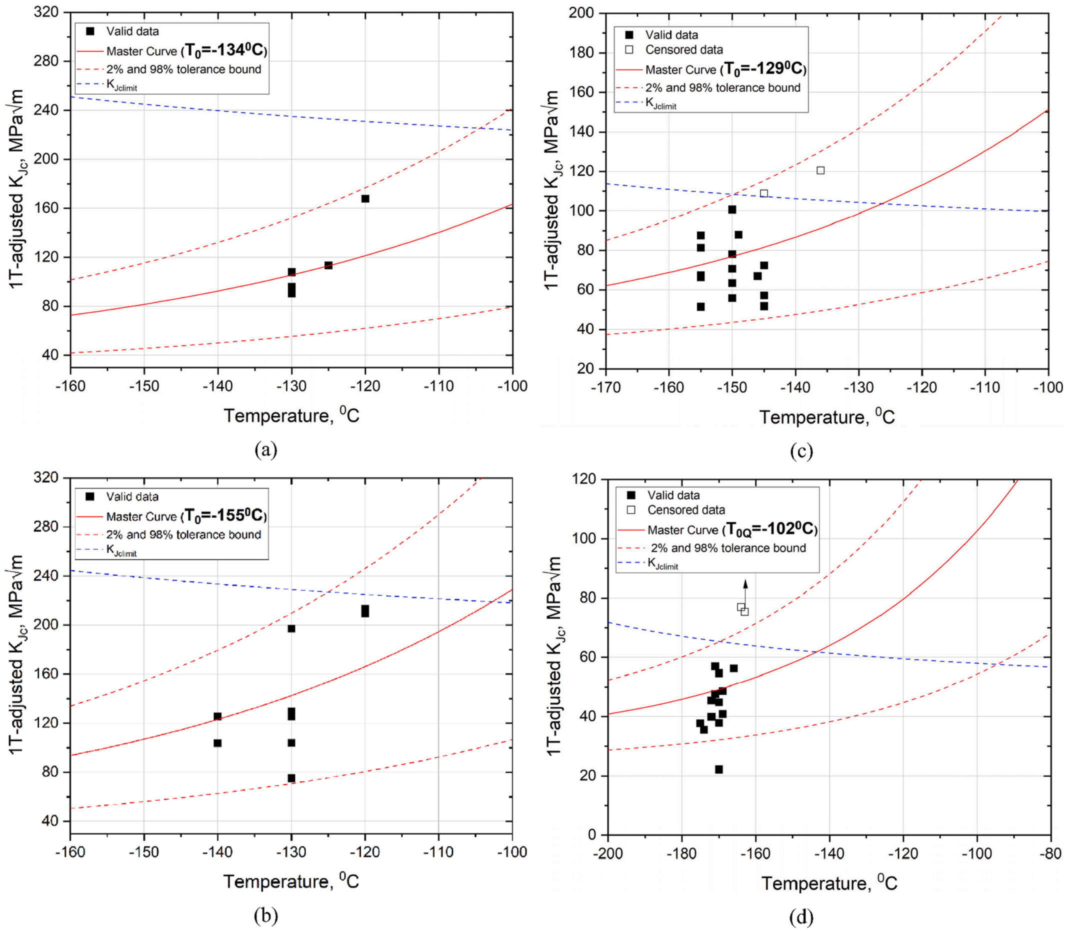

Fig. 3. Master curve fracture toughness results for F82H-BA12 (a) ORNL 0.5 T C(T), (b) CIEMAT 0.5 T C(T) (c) 4 mm miniC(T), and (d) 1.65 mm bend bar.

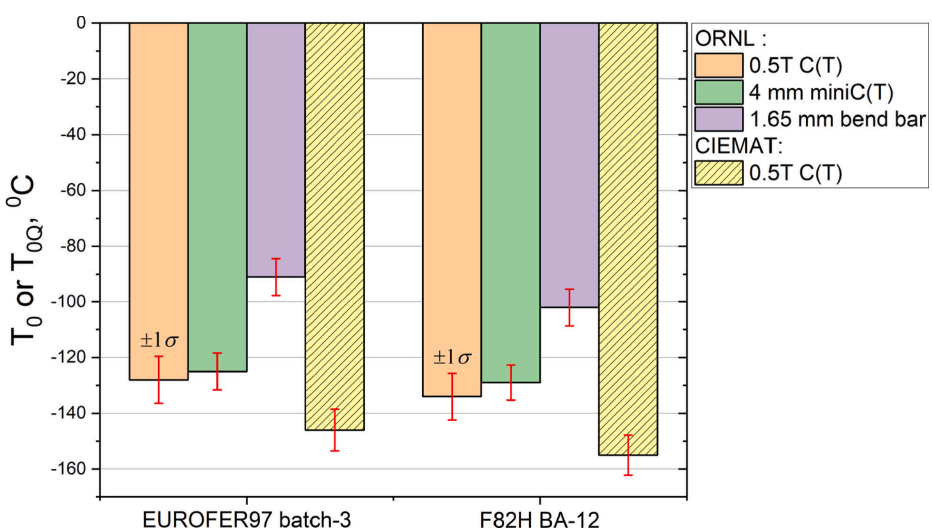

Fig. 4. Comparison of the Master Curve reference temperature T_{0Q} among three different specimen sizes.

The maximum fatigue force P_{max} was less than the control force P_m (See ASTM E1921-21 Eqs. (3) and (4)).

The average fatigue precrack size over width ratio (a_0/W) was within 0.45–0.55.

Any of the nine measurements of fatigue precrack met the crack extension requirements (See ASTM E1921-21 Fig. 5 and Table 2).

Any of the seven inner measurements of the fatigue precrack size differed by no more than $0.1(b_0B_N)^{1/2}$ from the average precrack size a_0, where b_0 is the initial uncracked ligament size and B_N is the specimen net thickness (equal to the specimen thickness B since all specimens were not side-grooved).

After fatigue precracking, fracture toughness testing was performed using a quasi-static loading rate such that dK/dt during the initial elastic loading portion was between 0.1 and 2 MPa$\sqrt{m}$/s. Testing temperatures

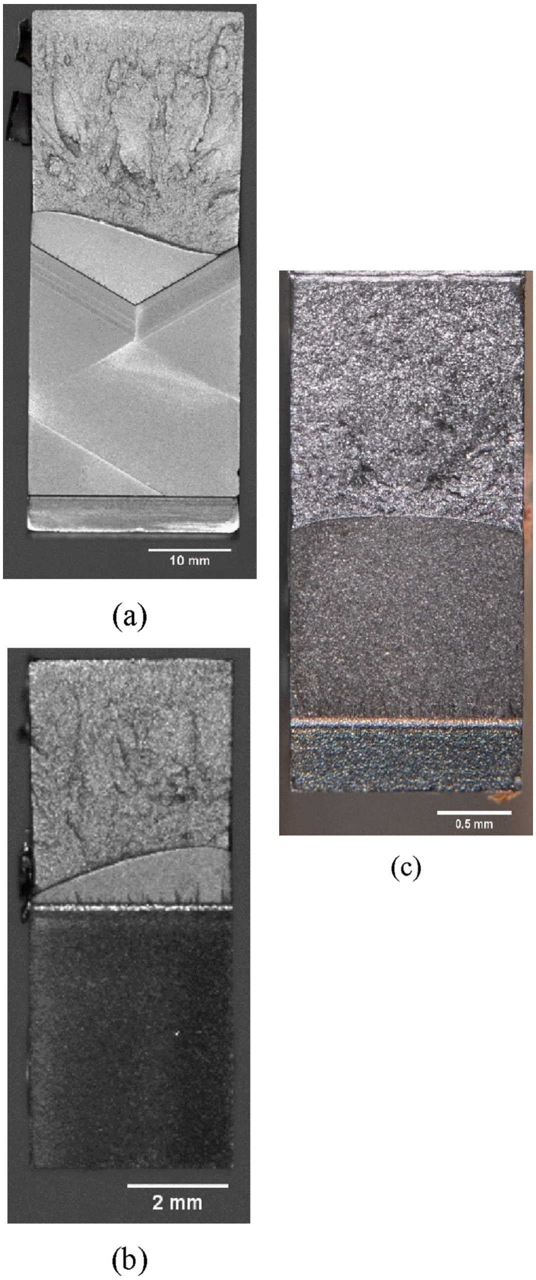

Fig. 5. Slanted fatigue precrack fronts observed in early ORNL campaign for (a) 0.5 T C(T) and (b) 4 mm miniC(T) whereas straight fatigue precrack fronts observed in (c) 1.65 mm bend bar specimens.

were chosen such that the median stress intensity factor $K_{Jc(med)}$ at the test temperature was about 100 MPa$\sqrt{m}$ for the specimen size selected. For 1.65 mm bend bar specimens, this was not possible due to the small fracture toughness capacity ($K_{Jclimit}$ defined in Equation (1)) inherent to the specimen type. Hence, lower testing temperatures had to be selected.

$$K_{Jclimit} = \sqrt{\frac{Eb_0\sigma_{YS}}{30(1-\nu^2)}} \quad (1)$$

where:
E = Young's modulus at the test temperature,
b_0 = the initial uncracked ligament size,
σ_{YS} = yield strength at the test temperature,
ν = Poisson's ratio (ν = 0.3).

Each specimen was tested until either cleavage occurred or the displacement gauge travel limit was reached. Then the crack size was measured from the fracture surface. The equivalent elastic–plastic stress intensity factor K_{Jc} was derived from the J-integral at the onset of cleavage fracture, J_c, using:

$$K_{Jc} = \sqrt{J_c\frac{E}{1-\nu^2}} \quad (2)$$

Then K_{Jc} was size-adjusted to 1 T (one-inch thickness) value based on the statistical weakest-link theory:

$$K_{Jc(1T)} = 20 + [K_{Jc(0)} - 20](\frac{B_0}{B_{1T}})^{1/4} \quad (3)$$

where:
$K_{Jc(1T)} = K_{Jc}$ for a thickness of one inch (B_{1T} = 25.4 mm),
$K_{Jc(0)} = K_{Jc}$ for a specimen thickness of B_0.

To calculate the Master Curve provisional reference temperature T_{0Q}, the multi-temperature analysis formula in Equation (4) was applied, and K_{Jc} data were censored against both the fracture toughness capacity limit $K_{Jclimit}$ and the slow stable crack growth limit $K_{Jc\Delta a}$.

$$\sum_{i=1}^{N}\delta_i\frac{\exp[0.019(T_i - T_{0Q})]}{11.0 + 77\exp[0.019(T_i - T_{0Q})]} - \sum_{i=1}^{N}\frac{(K_{Jc(i)} - 20)^4\exp[0.019(T_i - T_{0Q})]}{\{11.0 + 77\exp[0.019(T_i - T_{0Q})]\}^5} = 0 \quad (4)$$

where:
N = number of specimens tested,
T_i = test temperature corresponding to $K_{Jc(i)}$,
$K_{Jc(i)}$ = either a valid K_{Jc} datum or a datum replaced with a censoring value,
δ_i = 1.0 if the datum is valid or 0 if the datum is a censored value,
T_{0Q} = Master Curve provisional reference temperature obtained iteratively.

3. Results and discussion

3.1. Specimen size effect on Master Curve reference temperature T_0

The transition fracture toughness results of EUROFER97 batch-3 and F82H-BA12 are shown in Fig. 2 and Fig. 3, respectively. Results are compared between 0.5 T C(T), 4 mm miniC(T), and 1.65 mm bend bars. Also shown in the same figures are the curves for Master Curves fracture toughness given by:

$$K_{Jc(med)} = 30 + 70\exp[0.019(T - T_{0Q})] \quad (5)$$

where:
$K_{Jc(med)}$ = median fracture toughness for a multi-temperature data set of 1 T specimens,
T = test temperature,

The fracture toughness capacity limits $K_{Jclimit}$ is calculated from Equation (1), and the tolerance bounds are calculated using the following equation:

$$K_{Jc(0.xx)} = 20 + [\ln(\frac{1}{1-0.xx})]^{1/4}\{11 + 77\exp[0.019(T - T_{0Q})]\} \quad (6)$$

where:
0.xx = selected cumulative probability level, e.g., for the 2% tolerance bound, 0.xx = 0.02.

Fig. 2 and Fig. 3 show that the Master Curve reasonably predicts the median fracture toughness for the test temperature range. In addition, most valid data are bounded by the tolerance bounds indicating that the experimental toughness scatter was within the statistical prediction of the Master Curve method. Per ASTM E1921-21 standard [8], the testing temperature should be within ± 50 °C from the Master Curve reference temperature T_{0Q}. This requirement was met for 0.5 T C(T) and 4 mm miniC(T) specimens, while the testing temperatures for the 1.65 mm

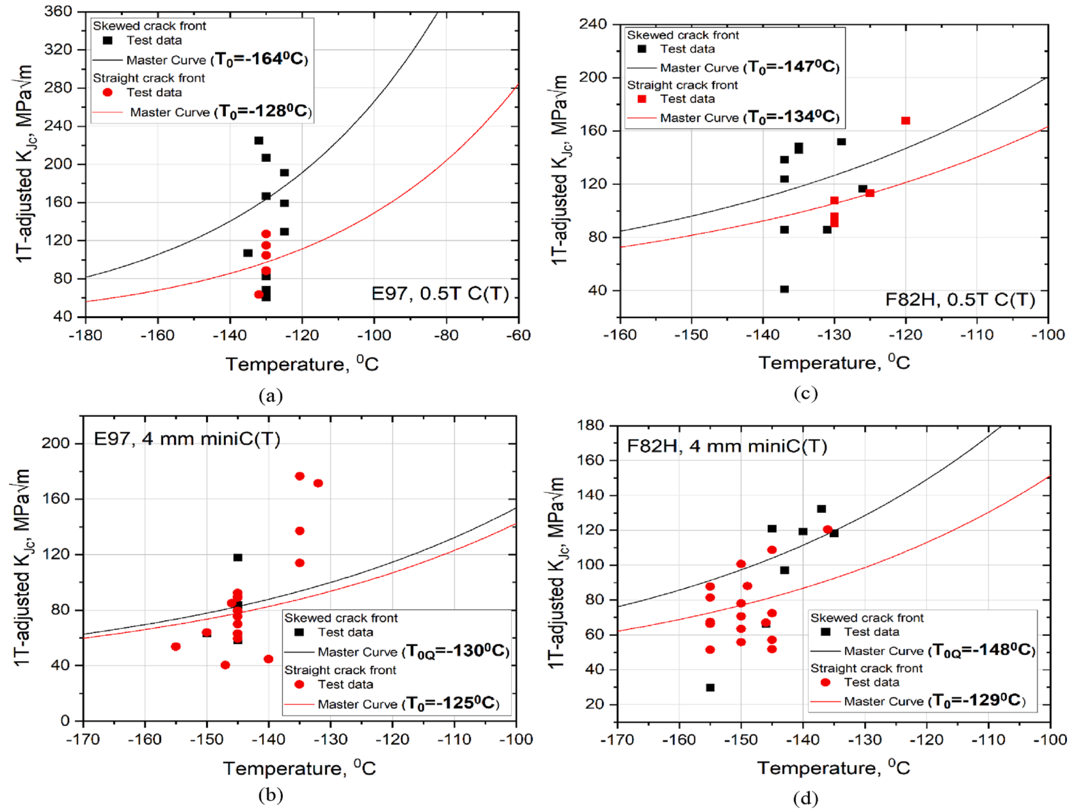

Fig. 6. Effect of fatigue precracking on Master Curve Reference temperature T_{0Q}.

bend bar were more than 50 °C lower than the derived T_{0Q} due to the inherently low $K_{Jclimit}$ of the bend bar. Nevertheless, the comparison of T_{0Q} obtained from three specimen types is still meaningful in the sense of providing data to support the ongoing activities within the ASTM E1921 task force to further widen the low test temperature window in Master Curve testing. The derived T_0 from 0.5 T C(T) and 4 mm miniC(T) specimens and T_{0Q} from 1.65 mm bend bars for the EUROFER97 batch-3 and F82H-BA12 are compared in Fig. 4. Very little differences were observed in T_0 between the ORNL 0.5 T C(T) and 4 mm miniC(T) specimens whereas CIEMAT 0.5 T C(T) T_0 was approximately 20 °C lower than that from ORNL 0.5 T C(T). However, considering ± one standard deviation (±1σ), the differences observed in T_0 between ORNL 0.5 T C(T) and CIEMAT 0.5 T C(T) were within a reasonable range. The overall observation indicates no size effect for 0.5 T C(T) and 4 mm miniC(T) specimens on T_0. This observation is in line with the literature findings on EUROFER97 [18] and F82H [19–25]. However, as shown in Fig. 4, for both EUROFER97 batch-3 and F82H-BA12, T_{0Q} from 1.65 mm bend bar specimens was higher than T_0 obtained from larger size specimens. This observation contradicts earlier results reported by Sokolov et al. [26,27] for F82H IEA heat but is in agreement with the works by Serrano et al. who reported higher T_0 for small size bend bar specimens of EUROFER97 batch-1 [28]. In addition, it is worth noting that this observation was in the opposite direction as the normally observed bias in T_0 between C(T) and SE(B) geometries. Further study is needed to understand the potential specimen size effect of bend bars.

3.2. Effect of fatigue precracking on the Master Curve reference temperature T_0

In the 1st batch testing at ORNL, we observed slanted fatigue precrack fronts in 0.5 T C(T) and 4 mm miniC(T) specimens, whereas straight fatigue precrack fronts were observed in all 1.65 mm bend bars as shown in Fig. 5. This observation holds for both EUROFER97 batch-3 and F82H-BA12. It was later determined that a slight misalignment in the fatigue frame load train contributed to the slanted fatigue precrack fronts for 0.5 T C(T) and 4 mm miniC(T) specimens, while 1.65 mm bend bars were probably spared from this issue due to a different type of fixture used in fatigue precracking (3-point bend type for 1.65 mm bend bars vs. clevis type for 0.5 T C(T) and 4 mm miniC(T) specimens). While the slanted fatigue precrack front violates the ASTM E1921-21 standard requirements on fatigue precrack front straightness and minimum crack extension from the machined notch root, analyses on the affected specimens were performed to evaluate the effect of fatigue precracking straightness on the Master Curve Reference temperature T_0. As shown in Fig. 6, the slanted fatigue precrack front resulted in unrealistically low T_{0Q} values from the affected 0.5 T C(T) and 4 mm miniC(T) specimens compared with the same size specimens with qualified straight fatigue precrack front. The root cause for the lower T_{0Q} values is that the Master Curve method in the ASTM E1921-21 standard assumes a sharp straight fatigue precrack front as a premise for the following fracture toughness testing. A slanted fatigue precrack front without sufficient crack extension from the machined notch root would result in a different stress field ahead of the fatigue precrack tip and artificially increase the material fracture toughness which ultimately leads to a lower T_{0Q}. In addition, the crack front portion without sufficient fatigue precrack would result in lower constraint which would affect the ensuring fracture toughness results as well.

After observing the slanted fatigue precrack fronts in 0.5 T C(T) and 4 mm miniC(T) specimens in the 1st batch, we implemented improvement on load train alignment. In detail, we reduced the number of components between the upper and lower load trains, applied fatigue grade lock washers with machined flat surfaces, adopted a new pair of clevis grips, and used spiral washers to preload the fatigue frame to minimize misalignment. Afterward, we performed 2nd batch testing of 0.5 T C(T) and 4 mm miniC(T) specimens at ORNL. The effect of fatigue load train alignment improvement on the fatigue precrack front straightness was apparent for 0.5 T C(T) and 4 mm miniC(T) specimens, as highlighted in Fig. 7. In summary, we significantly increased the

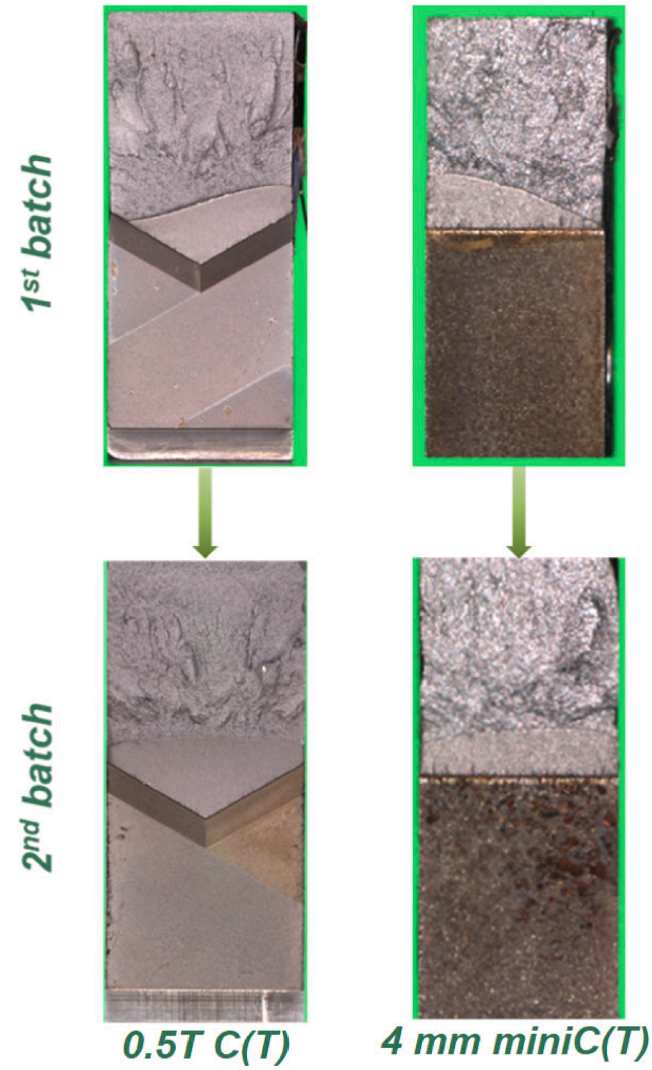

Fig. 7. Improvement on fatigue precrack front straightness after fatigue load frame alignment adjustment.

Table 2
Fatigue precrack success rate (%) per ASTM E1921-21 standard before and after the fatigue load train alignment improvement.

	0.5 T C(T)	4 mm miniC(T)	1.65 mm bend bar
Before improvement	0	50	100
After improvement	63	96	–

Table 3
Minimum number of uncensored tests required to yield a valid Master Curve reference temperature T_0 per ASTM E1921-21 [8].

(Test temperature - T_0) range °C	1 T $K_{Jc(med)}$ range MPa$\sqrt{m}$	Minimum number of uncensored tests
50 to −14	212 to 84	6
−15 to −35	83 to 66	7
−36 to −50	65 to 58	8

fatigue precrack success rate per ASTM E1921-21 standard for 0.5 T C(T) and 4 mm miniC(T) specimens (Table 2). It is worth mentioning that the fatigue precracking success rate was much higher in 4 mm miniC(T) specimens than in 0.5 T C(T) specimens as the Chevron notch adopted in

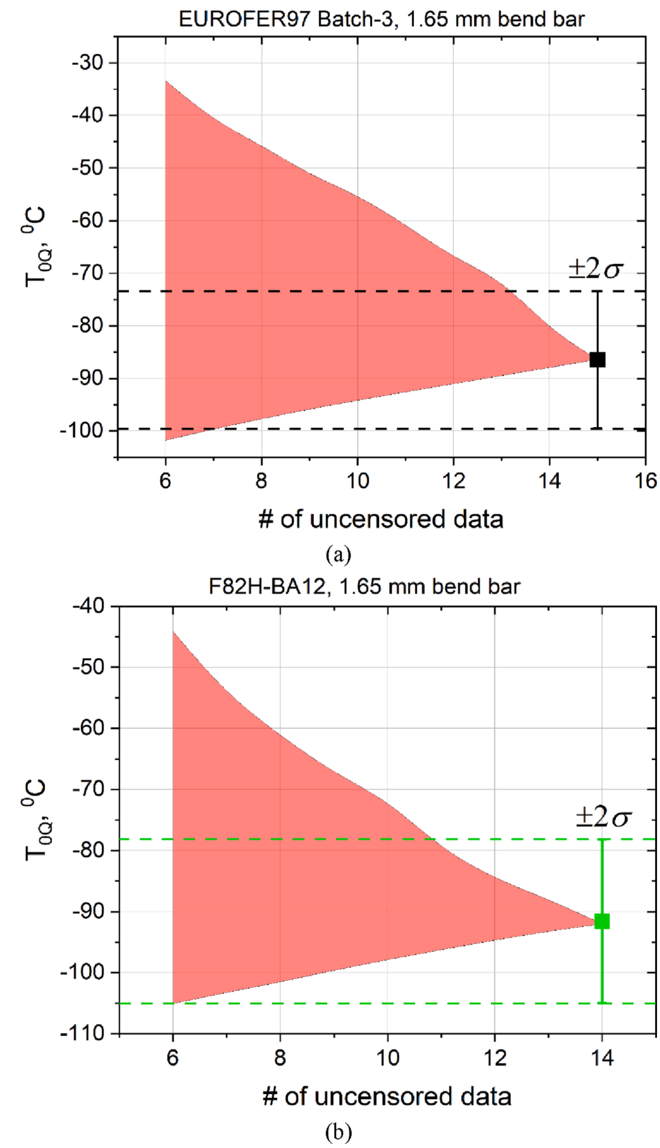

Fig. 8. The range of T_{0Q} with respect to the uncensored data sample size for 1.65 mm bend bar testing for EUROFER97 batch-3 in (a) and F82H-BA12 in (b). The black and green square symbols represent the $T_{0Qfinal}$ for EUROFER97 batch-3 and F82H-BA12, respectively. (For interpretation of the references to colour in this figure legend, the reader is referred to the web version of this article.)

0.5 T C(T) would render much shorter crack extension near both sides of a specimen, therefore not fulfilling the minimum crack extension requirement for the two side measurements (See ASTM E1921-21 Fig. 5 and Table 2). The 4 mm miniC(T) adopted a narrow straight notch and was not suggested to such an issue. In addition, there is still room for further fatigue precracking improvement, including turning specimens around in relation to the clevis grips at the middle point of fatigue precracking, replacing the Chevron notch with the straight notch for 0.5 T C(T), using only spiral washers, etc. It is worth noting that the 0.5 T C (T) and 4 mm miniC(T) results presented in the previous section are only derived from specimens with ASTM-qualified fatigue precracks.

3.3. Recommended minimum number of specimens per each specimen geometry

For experiment planning and material qualification purposes, one important aspect for Master Curve fracture toughness characterization, especially for irradiated materials, is to determine the minimum number of specimens needed for yielding a reliable T_0 for the investigated specimen type. For both 0.5 T C(T) and 4 mm miniC(T) specimens, testing and analysis can be performed in full compliance with the ASTM E1921-21 standard, and the minimum number of uncensored tests is shown in Table 3 according to ASTM E1921-21 [8].

The situation is more complicated for the 1.65 mm bend bar specimens, since 1 T $K_{Jc(med)}$ from this specimen type is usually less than 58 MPa$\sqrt{m}$ and the testing temperatures are more than 50 °C lower than T_{0Q} (e.g., Fig. 2d and Fig. 3d). Therefore, the ASTM E1921-21 requirement based on the test temperature range (see Table 3) is not applicable, and we are proposing a new approach based on random sampling in this study. For both EUROFER97 batch-3 and F82H-BA12, 16 bend bars were tested per material with 15 uncensored tests for EUROFER97 batch-3 and 14 uncensored tests for F82H-BA12. From the entire uncensored data population, a smaller data sample can be retrieved and used to calculate T_{0Q} and for the same sample size, there is a definite number of combinations of such sampling which can be used to calculate the range of T_{0Q}. For instance, for a population size of 15 and a sample size of 1, there are 15 possible combinations of sampling. The possible combinations increase to 5,005 for a population size of 15 and a sample size of 6. As the sample size increases, the calculated T_{0Q} range would approach a constant value corresponding to T_{0Q} calculated with the entire uncensored data population (referred to as $T_{0Qfinal}$ hereafter). The minimum uncensored tests for 1.65 mm bend bar specimens should correspond to the smallest uncensored sample size such that for this sample size and beyond, the calculated T_{0Q} range should be within $T_{0Qfinal} \pm 2\sigma$ where the standard deviation, σ, is calculated as:

$$\sigma = \sqrt{\frac{\beta^2}{r} + \sigma_{\exp}^2} \quad (7)$$

where:

β = sample size uncertainty factor, chosen as 20.1 °C corresponding to a 1 T $K_{Jc(med)}$ of 58 MPa$\sqrt{m}$ per the ASTM E1921-21 standard,

r = total number of uncensored data used to establish the value of T_{0Q},

σ_{exp} = contribution of experimental uncertainties, chosen as 4 °C per ASTM E1921-21 standard,

Fig. 8 shows the range of T_{0Q} with respect to the uncensored data sample size for 1.65 mm bend bar testing for EUROFER97 batch-3 and F82H-BA12. The smallest uncensored sample size was chosen as six, since the ASTM E1921-21 standard requires a minimum of six uncensored data for T_0 determination regardless of specimen size. Based on the aforementioned criterion, 13 uncensored tests are needed for EUROFER97 batch-3 T_{0Q} calculation and 11 are needed for F82H-BA12. On average, the minimum uncensored tests for the evaluation of T_{0Q} for 1.65 mm bend bar specimens are determined as 12. This applies to a testing temperature range for T-T_{0Q} from −50 °C to −80 °C. The result would provide guidance for the future application of 1.65 mm bend bar specimens for characterizing material transition fracture toughness.

4. Conclusions

EUROFER97 and F82H are two leading RAFM steels for fusion blanket applications. Commercialization of fusion technology requires in-depth understanding of materials post-irradiation behavior, including fracture toughness properties, for the safe long-term operation of fusion reactors. Due to the space constraint of irradiation facilities, the development of SSTT is necessary to evaluate the performance of irradiated materials. In this study, we evaluated the specimen size effect, the impact of fatigue precracking, and the minimum number of specimens required for Master Curve fracture toughness characterization of EUROFER97 batch-3 and F82H-BA12 steels. The main findings are:

(1) The current ASTM E1921 Master Curve and its tolerance bounds provide an excellent representation of the transition fracture toughness for EUROFER97 batch 3 and F82H-BA12.
(2) Considering ± one standard deviation (±1σ), there was no obvious specimen size effect in 0.5 T C(T) and 4 mm miniC(T) specimens on measured Master Curve reference temperature T_0, while 1.65 mm bend bar specimens yielded a higher (more conservative) T_{0Q} for both steels.
(3) Experimental quality control is critical for yielding valid Master Curve results. Small misalignments in the fatigue frame load train can result in slanted fatigue precrack fronts in 0.5 T C(T) and 4 mm miniC(T) specimens. In that regard, unrealistically low T_{0Q} values were derived from the affected specimens. Successful measures were taken to improve the fatigue frame alignment resulting in straight fatigue precrack fronts.
(4) The minimum number of specimens needed for 0.5 T C(T) and 4 mm miniC(T) testing can be determined per ASTM E1921-21 standard, while a minimum of 12 uncensored tests are recommended for 1.65 mm bend bar testing.

CRediT authorship contribution statement

Xiang Frank Chen: Conceptualization, Methodology, Formal analysis, Validation, Investigation, Resources, Visualization, Project administration, Writing – original draft. **Marta Serrano:** Methodology, Formal analysis, Validation, Investigation, Project administration, Resources, Writing – review & editing, Funding acquisition. **Rebeca Hernández:** Investigation, Methodology, Formal analysis, Investigation, Writing – review & editing. **Dan Lu:** Methodology, Formal analysis, Writing – review & editing. **Mikhail A. Sokolov:** Investigation, Resources, Writing – review & editing, Supervision. **Sehila M. Gonzalez De Vicente:** Data curation, Resources, Project administration, Writing – review & editing, Funding acquisition. **Yutai Katoh:** Resources, Writing – review & editing, Supervision, Funding acquisition, Project administration.

Declaration of Competing Interest

The authors declare that they have no known competing financial interests or personal relationships that could have appeared to influence the work reported in this paper.

Data availability

Data will be made available on request.

Acknowledgments

This research at ORNL was sponsored by the U.S. Department of Energy, Office of Fusion Energy Sciences, under contract DE-AC05-00OR22725 with UT-Battelle, LLC. The research at CIEMAT was sponsored by EUROFusion Consortium agreement and the Euratom research and training program under grant No 633053. We also appreciate the support from the IAEA CRP F13017 "Towards the Standardization of Small Specimen Test Techniques for Fusion Applications". The views and opinions expressed herein do not necessarily reflect those of the International Atomic Energy Agency. The raw materials used in this study, EUROFER97 Batch-3 and F82H-BA12, were provided by Fusion for Energy (F4E) and National Institutes for Quantum Science and Technology (QST), respectively.

We appreciate contributions from the following personnel at ORNL: Eric Manneschmidt and Jordan Reed for performing fracture toughness testing; Doug Stringfield for facilitating specimen machining. Lastly, we would like to thank Tim Graening and TS Byun, also from ORNL, for their thoughtful review of this manuscript.

References

[1] K. Shiba, H. Tanigawa, T. Hirose, T. Nakata, Development of the toughness-improved reduced-activation F82H steel for DEMO reactor, Fusion Sci. Technol. 62 (1) (2012) 145–149.
[2] L. Tan, Y. Katoh, A.-A. Tavassoli, J. Henry, M. Rieth, H. Sakasegawa, H. Tanigawa, Q. Huang, Recent status and improvement of reduced-activation ferritic-martensitic steels for high-temperature service, J. Nucl. Mater. 479 (2016) 515–523.
[3] K. Shiba, M. Enoeda, S. Jitsukawa, Reduced activation martensitic steels as a structural material for ITER test blanket, J. Nucl. Mater. 329 (2004) 243–247.
[4] S. Jitsukawa, M. Tamura, B. Van der Schaaf, R. Klueh, A. Alamo, C. Petersen, M. Schirra, P. Spaetig, G. Odette, A. Tavassoli, Development of an extensive database of mechanical and physical properties for reduced-activation martensitic steel F82H, J. Nucl. Mater. 307 (2002) 179–186.
[5] A.-A. Tavassoli, J.-W. Rensman, M. Schirra, K. Shiba, Materials design data for reduced activation martensitic steel type F82H, Fusion Eng. Des. 61 (2002) 617–628.
[6] F. Garner, L. Greenwood, Neutron irradiation effects in fusion or spallation structural materials: some recent insights related to neutron spectra, Radiat Eff. Defects Solids 144 (1–4) (1998) 251–286.
[7] S.M. González de Vicente, J.L. Boutard, S.J. Zinkle, H. Tanigawa, Materials testing facilities and programmes for fission and ion implantation damage, Nucl. Fusion 57 (9) (2017), 092011.
[8] ASTM, ASTM E1921-21 Standard Test Method for Determination of Reference Temperature, To, for Ferritic Steels in the Transition Range, ASTM International, West Conshohocken, PA, 2021, p. 39.
[9] L. Commin, S. Baumgärtner, B. Dafferner, S. Heger, M. Rieth, A. Möslang, Creep-Fatigue Interaction in Eurofer 3 Electron Beam Welds, Fusion Sci. Technol. 66 (1) (2014) 131–135.
[10] X. Chen, M.A. Sokolov, S.M. Gonzalez De Vicente, Y. Katoh, Specimen Size and Geometry Effects on the Master Curve Fracture Toughness Measurements of EUROFER97 and F82H Steels, Proceedings of the . Volume 1: Codes and Standards. Las Vegas, Nevada, USA. July 17–22, 2022. V001T01A048. ASME. https://doi.org/10.1115/PVP2022-84514.
[11] A. Möslang, E. Diegele, M. Klimiankou, R. Lässer, R. Lindau, E. Lucon, E. Materna-Morris, C. Petersen, R. Pippan, J. Rensman, Towards reduced activation structural materials data for fusion DEMO reactors, Nucl. Fusion 45 (7) (2005) 649.
[12] X. Chen, R. Hernandez Pascual, M. Serrano, D. Andres, H. Nolles, M.A. Sokolov, Guidelines for IAEA Small Specimen Test Techniques Master Curve Fracture Toughness Testing, United States (2020), https://doi.org/10.2172/1649107.
[13] X. Chen, M.A. Sokolov, A. Bhattacharya, L.N. Clowers, T. Graening, Y. Katoh, M. Rieth, Master Curve Fracture Toughness Characterization of Eurofer97 Steel Variants Using Miniature Multi-Notch Bend Bar Specimens for Fusion Applications, Proceedings of the . Volume 1: Codes and Standards. San Antonio, Texas, USA. July 14–19, 2019. V001T01A036. ASME. https://doi.org/10.1115/PVP2019-93797.
[14] X. Chen, M.A. Sokolov, Y. Katoh, M. Rieth, L.N. Clowers, Master Curve Fracture Toughness Characterization of Eurofer97 Using Miniature Multi-Notch Bend Bar Specimens for Fusion Applications, Volume 1A: Codes and Standards. Prague, Czech Republic. July 15–20, 2018. V01AT01A076. ASME. https://doi.org/10.1115/PVP2018-85065.
[15] X. Chen, M.A. Sokolov, K.D. Linton, L.N. Clowers, Y. Katoh, Transition Fracture Toughness Characterization of Eurofer 97 Steel using Pre-Cracked Miniature Multi-notch Bend Bar Specimens, United States (2017), https://doi.org/10.2172/1414686.
[16] X. Chen, A. Bhattacharya, M.A. Sokolov, L.N. Clowers, Y. Yamamoto, T. Graening, K.D. Linton, Y. Katoh, M. Rieth, Mechanical properties and microstructure characterization of Eurofer97 steel variants in EUROfusion program, Fusion Eng. Des. 146 (2019) 2227–2232.
[17] X.F. Chen, M.A. Sokolov, J. Robertson, M. Ando, J.W. Geringer, H. Tanigawa, Y. Katoh, Effects of HFIR neutron irradiation on fracture toughness properties of standard and Ni-doped F82H, J. Nucl. Mater. 542 (2020), 152501.
[18] D. Andres, M. Serrano, R. Hernandez, Y. Wang, M. Richardson, Determination of Eurofer97 Fracture Toughness by Testing Small C(T) Specimens, Proceedings of the . Volume 1: Codes and Standards. Virtual, Online. July 13–15, 2021. V001T01A025. ASME. https://doi.org/10.1115/PVP2021-62040.
[19] W. Han, K. Yabuuchi, R. Kasada, A. Kimura, E. Wakai, H. Tanigawa, P. Liu, X. Yi, F. Wan, Application of small specimen test technique to evaluate fracture toughness of reduced activation ferritic/martensitic steel, Fusion Eng. Des. 125 (2017) 326–329.
[20] B.J. Kim, R. Kasada, A. Kimura, E. Wakai, H. Tanigawa, Application of master curve method to the evaluation of fracture toughness of F82H steels, J. Nucl. Mater. 442 (1–3 SUPPL.1) (2013) S38–S42.
[21] B.J. Kim, R. Kasada, A. Kimura, H. Tanigawa, Specimen size effects on fracture toughness of F82H steel for fusion blanket structural material, Green Energy Technol. (2011) 286–291.
[22] B.J. Kim, R. Kasada, A. Kimura, H. Tanigawa, Effects of specimen size on fracture toughness of phosphorous added F82H steels, Fusion Eng. Des. 86 (9–11) (2011) 2403–2408.
[23] T. Yamamoto, G. Odette, D. Gragg, H. Kurishita, H. Matsui, W. Yang, M. Narui, M. Yamazaki, Evaluation of fracture toughness master curve shifts for JMTR irradiated F82H using small specimens, J. Nucl. Mater. 367 (2007) 593–598.
[24] M. Sokolov, H. Tanigawa, Application of the master curve to inhomogeneous ferritic/martensitic steel, J. Nucl. Mater. 367 (2007) 587–592.
[25] M.A. Sokolov, H. Tanigawa, Application of the master curve methodology to fracture toughness characterization of ferritic-martensitic steel, 11th International Conference on Fracture 2005, ICF11, 2005, pp. 4194-4198.
[26] M. Sokolov, H. Tanigawa. Fusion Reactor Materials Program Semiannual Progress Report, 2002, p. 105.
[27] M. Sokolov, H. Tanigawa. Fusion Reactor Materials Program Semiannual Progress Report, 2006, p. 83.
[28] M. Serrano, P. Fernández, J. Lapeña, Fracture toughness evaluation of eurofer97 by testing small specimens, J. ASTM Int. 5 (4) (2008).